

Taguchi-RBF Neural networks Based Optimization of Phased Array Antenna With Coupling Effects

K. Oureghi¹, R. Ghayoula^{1,2}, W. Amara³, A. Smida^{1,4}, I. El Gmati⁵ and J. Fattahi⁶

¹Microwave Electronics Research Laboratory, Faculty of Mathematical, Physical and Natural Sciences of Tunis, Tunis El Manar University, Tunis 2092, Tunisia

²Faculté d'ingénierie - Université de Moncton, New Brunswick, NB E1A 3E9, Canada

³SysCom Laboratory, ENIT, University of Tunis El Manar, Tunis 1068, Tunisia

⁴Department of Medical Equipment Technology, College of Applied Medical Sciences, Majmaah University, Almajmaah 11952, KSA

⁵College of Engineering at Al Gunfudha Umm Al Qura University, KSA

⁶Department of Electrical and Computer Engineering, Laval University, Quebec City, QC G1V0A6, Canada

Correspondence: ridha.ghayoula.1@ulaval.ca (R.G.); iagmati@uqu.edu.sa (I.E.G.)

ABSTRACT In the antenna array synthesis problems, most of the works in literature utilize isotropic elements. Thus, the mutual coupling effects between the array elements are neglected. It is obvious that an array antenna synthesized by neglecting the coupling effects cannot be used in the real world applications due to the possible mismatch between the desired and realized radiation patterns. In this paper, a novel method based on neural network algorithm RBF (Radial Basis Function) for the synthesis and modeling of Antipodal Vivaldi antenna with mutual coupling effect is presented. The synthesis in implementation's method for this type of array permits to approach the appropriated radiation pattern while considering the mutual coupling between its elements. The neural network is used to estimate the array elements' excitations. The architecture of the neural network based on the radial basis functions (RBFs) is introduced and simulation results are presented. Results show that there is an agreement between the desired specifications and the synthesized one. The proposed optimization approach offers an efficient and robust synthesis procedure.

INDEX TERMS Taguchi-RBF Neural Networks, Mutual coupling, phased antenna array, radiation pattern

I. INTRODUCTION

ANTENNAS play a major role in the wireless communication systems. The performances of the antenna module can significantly enhance the performances of wireless communication systems such spectral and energy efficiencies. For some applications, the single element antenna is unsuitable because it does not meet the required gain and radiation patterns. Alternatively, we therefore combine the multiple element antennas to improve the overall performances and spectral efficiency of the wireless systems. When an object is placed in the vicinity of a radiating element, it will affect the current distribution of that element and in consequence the radiated fields. Therefore, the current of close elements together with own currents of the radiator alter the characteristics of the antenna. Energy exchange or electromagnetic interaction between the array elements of an antenna array is known as Mutual Coupling and is an unwanted effect. It complicates the antenna design and analysis, influences the radiation pattern of the whole array and is difficult to generalize[34]. In [1] a brief review of the decoupling methods for the mutual coupling effect in antenna arrays. In [2] a short review of the receiving-mutual-impedance method (RMIM) for mutual coupling compensation in direction find-

ing applications using linear array. Hoi Shun Lui and Hon Tat Hui used mutual coupling compensation for Direction-of-Arrival Estimations using the receiving-mutual-impedance method. Min Wang, Wen Wu, and Zhongxiang Shen [3] used a bandwidth enhancement of antenna arrays utilizing mutual coupling between antenna elements[5]. E. Saenz, K. Guven, E. Ozbay, I. Ederra, and R. Gonzalo have treated in [4] decoupling of multifrequency dipole antenna arrays for microwave imaging applications. Recently, many multiagent stochastic optimization techniques that incorporate random variation and selection, such as evolutionary programming(EPs)[6]-7], genetic algorithms (GA) [8]-[9], particle swarm optimization (PSO)[10]-[11], artificial neural network (ANN) [12]-[13], and gradient-based techniques [14]-[15], have been implemented via computer codes. The Vivaldi antenna has been used in many microwave engineering applications for its simple structure, low cross polarization, and highly directive patterns characteristics, especially in ultra bandwidth applications such as vehicular wireless communication, radar imaging, and through-the-wall imaging [16]-[17]. Many kinds of Vivaldi antennas have been investigated for wideband application [18]-[19], and some new antipodal Vivaldi antennas have been designed to improve radiation pattern and

directivity [20]-[21]-[33]. The use of numerical methods to obtain the radiation characteristics of two or more printed antennas involves significant computation time. When we want to design a network made up of such antennas, we want First, precisely size this network in terms of coupling and distance between antennas. We therefore try to develop simple and precise analytical formulations on the impedance and the coupling between the printed antennas. We begin by studying printed antennas, the main elements for the design of printed antennas. The results of this analytical study are validated by digital simulators according to the distance between antennas [36]-[37]-[38]. In this paper Taguchi-RBF is proposed to design linear antenna array for the a given optimum radiation pattern using Taguchi and radial basis function Neural Networks with the element's excitation and separation as the control parameters. Initially, the network is trained with a set of input-output data pairs. The trained network is used for testing. The training data set is generated from MATLAB simulation with number of elements $N = 8$ elements of linear array. Finally, electromagnetic simulations are performed using the CAD tool HFSS from ANSYS Inc. to validate the synthesized antenna design

The paper is organized as follows. The theoretical analysis and problem formulation using of mutual coupling is presented in section II. Antipodal Vivaldi antenna array design is developed in section III. Section IV shows Taguchi-RBF neural networks result.Finally,section V makes conclusions.

II. THEORETICAL ANALYSIS

Uniform arrays are widely used due to their relatively simple feeding system that can be designed in a systematic way. The downside of uniform arrays is the presence of grating lobes, due to the spatial periodicity. Grating lobes are other main lobes that appear in the radiation pattern besides the main lobe due to the aliasing. The analysis of the array factor, instead of the total far field array, is essential to predict the presence of grating lobes.

A. MUTUAL COUPLING IN ANTENNA ARRAYS

Mutual coupling is a common problem in the applications of antenna arrays [35]-[39]-[40]. It significantly affects the operation of almost all types of antenna arrays. Over the past years, there have been many different kinds of methods suggested to decouple the mutual coupling effect in antenna arrays[22]-[23]-[32]. Transmit Mode Analysis Clearly, the input characteristics at port 2 change due to what we connect at port 1. From this Figure we can write the following expressions v is defined by

$$v = \begin{bmatrix} v_1 \\ v_2 \end{bmatrix} = Z_A i \quad (1)$$

We can write v_1 and v_2 by these two expressions

$$v_1 = Z_{A,11}i_1 + Z_{A,12}i_2 \quad (2)$$

$$v_2 = Z_{A,21}i_1 + Z_{A,22}i_2 \quad (3)$$

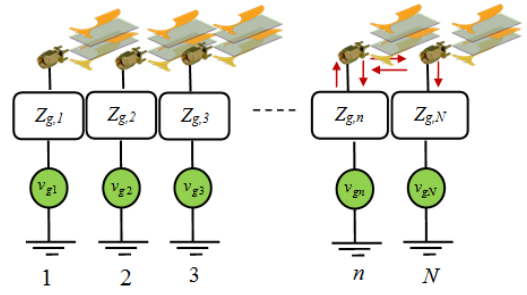


FIGURE 1. Mutual Coupling in Antenna Arrays

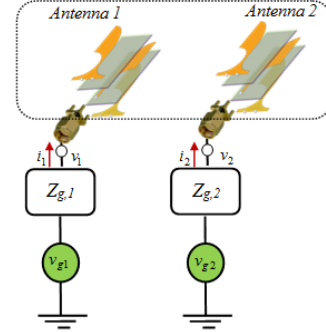


FIGURE 2. Coupling in transmitting mode

We can also describe

$$v_1 = v_{g1} - z_{g1}i_1 \quad (4)$$

$$v_{g1} - z_{g1}i_1 = Z_{A,11} + Z_{A,12}i_2 \quad (5)$$

We can deduce the analytic expressions of and with these equations

$$i_1 = \frac{v_{g1} - Z_{A,12}i_2}{Z_{A,11} + Z_{g1}} \quad (6)$$

and v_2 can then be expressed such that

$$v_2 = \underbrace{\frac{Z_{A,21}v_{g1}}{Z_{A,11} + Z_{g1}}}_{v_2^{oc}} + \underbrace{\left[Z_{A,22} - \frac{Z_{A,21}Z_{A,12}}{Z_{A,11} + Z_{g1}} \right]}_{Z_{in,2}} i_2 \quad (7)$$

To be able to transmit information at long distances, the antenna has to be highly directive. While a single antenna usually has a broad radiation pattern and a low directivity, a linear array of antennas can achieve a narrower pattern and higher directivity through the Array Factor. This factor quantifies the combination of radiating elements without taking into account the radiation pattern of the single element. Soon after the computation of mutual impedance for each antenna element of an array based on the above procedure, the calculation of array radiation pattern in mutual coupling environment can be done by modeling the array excitation as a set of Thevenin equivalent voltage sources with non-zero source impedances $Z_{g,n}$ as shown in Fig.1 The active input impedance Z_{an} due to the effect of mutual coupling. If v_{gn}

is the feed voltage, then the resulting feed current i_n will be given by applying Kirchoff's voltage law:

$$i_n = \frac{v_g}{Z_{an} + Z_{g,n}} \quad (8)$$

It is clear that resulting current feed kept on varying depending on the value of active input impedance Z_{an} . If it is assumed that an identical voltage source is applied to each element, then the generator impedances $Z_{gn} = Z_n$ with $v_g = v$ for all n , where Z_g is the universal generator impedance. Thus, the expression for i_n can be re-written as:

$$i_n = \frac{v}{Z_{an} + Z_g} \quad (9)$$

Under conditions neglecting the effect of mutual coupling, the expression for voltage source will be given as:

$$v = i \times Z_g \quad (10)$$

Where i is the current flowing through each antenna element in above condition. The expression for current excitation with mutual coupling effects solely depends on active input impedance as given under

$$i_n = i \times \frac{Z_g}{Z_{an} + Z_g} \quad (11)$$

Let us consider the array factor AF expression for a general linear array antenna without mutual coupling

$$AF(\theta, \phi) = \sum_{n=1}^N i_n e^{j[(n-1)kd \cos \theta + \beta]} \quad (12)$$

When considering the mutual coupling between antennas the AF expression becomes:

$$AF_{mut}(\theta, \phi) = \sum_{n=1}^N i \times \frac{Z_g}{Z_{an} + Z_g} \times e^{j[(n-1)kd \cos \theta + \beta]} \quad (13)$$

thus,

$$AF_{mut}(\theta, \phi) = Z \times AF(\theta, \phi) \quad (14)$$

Where,

Z is impedance

$\frac{Z_g}{Z_{an} + Z_g}$ is the Impedance Factor due to mutual coupling.

Z_g is the generator impedance or self impedance of antenna element.

Z_{an} is the active input impedance or mutual-impedance of nth antenna element.

B. RECEIVE MODE ANALYSIS

The mechanism of mutual coupling in receiving mode is shown in Fig. 3. Assume that a plane wave is incident, and it strikes antenna 1 first where it causes current flow. Part of the incident wave will be re-scattered into space, the other will be directed toward antenna 2 where it will add vectorially with the incident wave, and part will travel into its feed. It is then evident that the amount of energy received by each

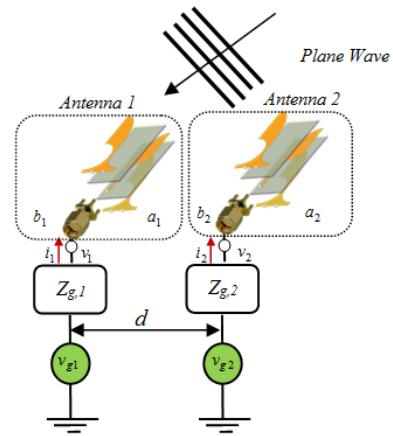


FIGURE 3. Coupling in receiving mode

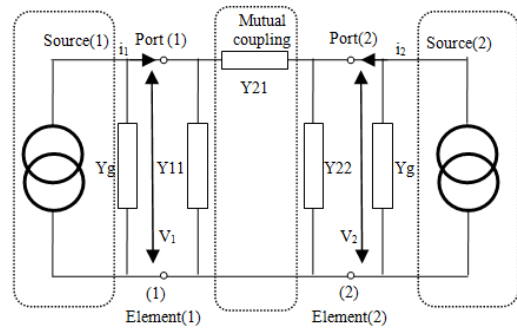


FIGURE 4. Y-network for two identical array elements.

element of an antenna array is the vector sum of the direct waves and those that are coupled to it parasitically from the other elements[5]. The effects of the mutual coupling on the performances of an array depends upon the

- antenna type and its design parameters.
- relative positioning of the elements in the array.
- feed of the array elements.
- scan volume of the array.

These design parameters influence the performances of the antenna array by varying its element impedance, reflection coefficients, and overall antenna pattern.

Consider an array of (N) identical elements separated by distance w_1, w_2, \dots, w_{N-1} with element pattern $f(\theta)$ and spacing between the (n) and ($n + 1$) element is w_n where $n = 1, 2, \dots, N$. Assuming no mutual coupling, the radiated field is [1]:

$$E \cong f(\theta) e^{-jkR} AF(\theta) \quad (15)$$

Where $AF(\theta)$ is the array factor and is equal to:

$$AF(\theta) = \sum_{n=1}^N V_n^{(0)} \exp \left[jk \left(\sum_{i=1}^{N-1} w_i \right) \sin \theta \right] \quad (16)$$

and k is the free space wave number and R, θ are the spherical coordinates.

For the case of mutual coupling, consider the Y-network given in Fig. 4 for two identical antenna elements. The actual

excited voltage V_1 is equal to the applied voltage $V_1^{(0)}$ plus that excited by the mutual coupling and is equal to

$$V_1 = V_1^{(0)} - \frac{Y_{12}}{Y_{11} + Y_g} V_2 \quad (17)$$

Now, invoking superposition and neglecting higher order coupling

$$V_n = V_n^{(0)} - \sum_{m=1, m \neq n}^N C_{mn} V_n^{(0)} \quad (18)$$

C_{mn} is the mutual coupling factor and is equal to

$$C_{mn} = \frac{Y_{mn}}{Y_{mn} + Y_g}, C_{mm} = 0 \quad (19)$$

Where

Y_{mn} is the mutual admittance between the m th and n th elements.

Y_{11} is the self-admittance of the element at the feed terminals. Y_g is the generator or feed-line admittance.

We can write AF according to the following equations by

$$AF(\theta) = \sum_{n=1}^N V_n^{(0)} \exp \left[jk \left(\sum_{i=1}^{N-1} w_i \right) \sin \theta \right] - \sum_{n=1}^N \sum_{m=1, m \neq n}^N C_{mn} V_n^{(0)} \exp \left[jk \left(\sum_{i=1}^{N-1} w_i \right) \sin \theta \right] \quad (20)$$

The radiation Pattern

$$AF(\theta) = \sum_k AF_k^{oc}(\theta) i_k = AF_1^{oc} i_1 + AF_2^{oc} i_2 \quad (21)$$

Where

AF_k^{oc} : Pattern of k th antenna.

$$AF(\theta) = AF_2^{oc} i_2 - \frac{AF_1^{oc} Z_{A,12} i_2}{Z_{A,11}} = \underbrace{\left[AF_2^{oc} i_2 - \frac{Z_{A,12}}{Z_{A,11} + Z_{g1}} AF_1^{oc} \right]}_{AF_2^{oc'}(\theta)} i_2 \quad (22)$$

In this section, various approaches for mutual-coupling compensation have been developed. In general, the mutual-coupling problems for a transmitting and receiving array are different, even if the physical geometry of the array remains unchanged. However, it seems that antenna engineers are not well aware of such differences in the analysis of receiving antenna arrays. It is concluded that the mutual-coupling problems of transmitting and receiving arrays are in general different, and hence different mutual impedance should be used for mutual-coupling analysis and compensation.

III. ANTIPODAL VIVALDI ANTENNA ARRAY

Antipodal Vivaldi antenna is a type of tapered slot antenna which is an end fire antenna. The antenna consists of the feeding line and the transition and the radiating structures. In general, the radiated structure is exponentially or elliptically

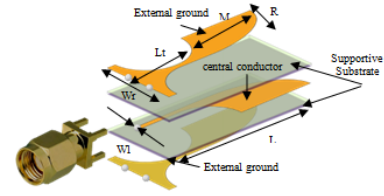


FIGURE 5. Designed Antipodal Vivaldi antenna

TABLE 1. Antenna Parameters(Antipodal Vivaldi antenna)

Parameters	(mm)
W	80
L	80
L_r	1.15
W_l	1.15
W_r	40
L_t	40
M	40
R	4.57

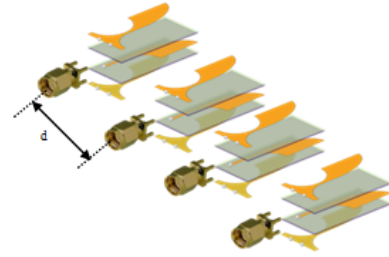


FIGURE 6. Antipodal Vivaldi antenna array

tapered, which means that they are composed of two layers. In this section an UWB antipodal Vivaldi antenna is presented. It is found that by inserting exponential slots into both patches of the antipodal Vivaldi antenna a good matching can be achieved, specially for the lower bandwidth limit, without degradation of the other performances of the proposed antenna. The characteristics of this antenna have been studied numerically using a commercial simulator ANSYS HFSS (High Frequency Electromagnetic Field Simulation). The design parameters and Antipodal element are shown in Fig.5. Exponential tapered profile is a common shape to obtain a relatively wide impedance bandwidth. The antenna was designed with FR4 (dielectric constant = 4.4, dielectric loss tangent = 0.02 and thickness=1.6 mm) to operate for UWB frequency 3.1 GHz – 10.6 GHz. The Fig.5 shows a 3D photograph of the antipodal Vivaldi antenna[24]-[41].

In order to provide evidence for the antenna effectiveness design, many parameters were simulated. The efficiency of the matching device is proved by the minimum return loss S_{11} , which influences the remnant characteristics such as Directivity, Gain and band width[25]. The antenna parameters are summarized in Table I.

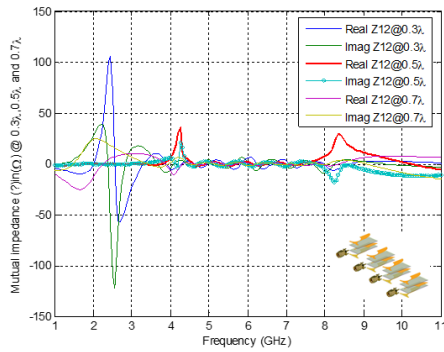


FIGURE 7. The receiving mutual impedance Z_{12} of two Antipodal Vivaldi antenna

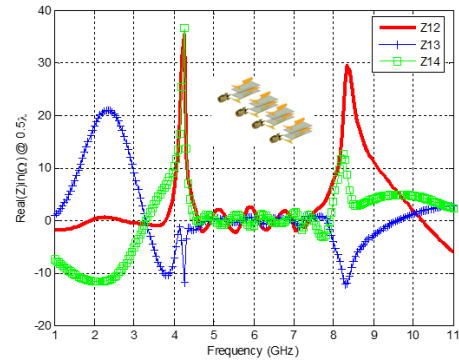


FIGURE 8. Mutual impedances Z_{12}, Z_{13} and Z_{14}

A. SIMULATIONS AND RESULTS

Validation of our analysis are demonstrated and discussed in this section defined as follow: Evaluating the accuracy of the matching impedance antenna resulting from simulating the return loss S_{11}, Z_{ij} and S_{ij} according to the distances between antennas. Simulating the effectiveness and extracting the antenna parameters, plotting , simulating a conventional linear antenna array and comparing results. In this work, Antipodal Vivaldi antenna are modeled in HFSS at a frequency of 5 GHz. The extent and nature of the effects of mutual coupling in different antennas array configurations are investigated by varying the inter-element and number of elements in linear antenna array pattern systematically. In this section, HFSS software is used for simulating the radiation patterns of antenna arrays and measuring the mutual coupling between the array elements. The mutual impedance for antenna array in receiving mode was redefined as receiving mutual impedance. Consider the Antipodal Vivaldi antenna array in Fig. 6. The two antennas are identical and lie in $x - z$ plane. An external source, coming from a direction of φ in the azimuth plane, excites the antennas. The receiving mutual impedance Z_{12} , between the antennas is defined as the ratio of the induced voltage V_1 , across the terminal load of antenna 1 to the current i_2 , on the terminal load of antenna 2 when the current on antenna 2 is excited by the external source.

$$Z_{12} = \frac{V_1}{i_2} \quad (23)$$

ANSYS HFSS software was used to study parameters of the proposed structure. Through parameters sweeps and optimization, the different values of inter-element distance ($0.3\lambda, 0.5\lambda$ and 0.7λ) were found important in this design. The results of parametric studies are depicted in Figs. 7,8 and 9.

Figs 10,11 and 12 show the mutual coupling coefficient, S_{12}, S_{13} and S_{14} as a function of resonance frequency for different values of inter-element distance ($0.3\lambda, 0.5\lambda$ and 0.7λ). The maximum mutual coupling is obtained at the minimum return loss for the same resonance frequency and the peaks are shifted to the direction of increasing frequency with increasing the inter-element distance. HFSS simulations

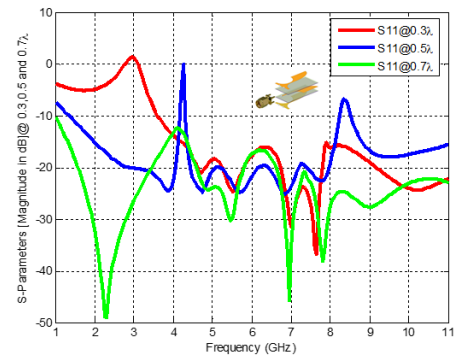


FIGURE 9. Reflection coefficient of the antenna with different values of inter-element distance ($0.3\lambda, 0.5\lambda$ and 0.7λ)

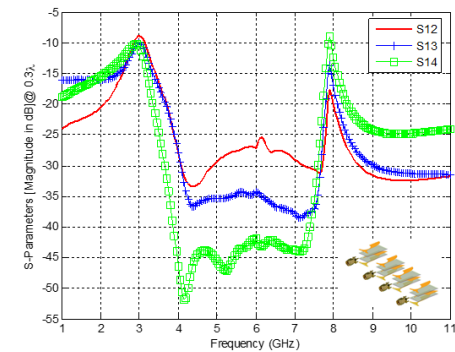


FIGURE 10. Parametric study of the broadband mutual coupling for different values of inter-element distance (0.3λ) (4 antennas array)

are performed to analyze and compare the S-parameters and their radiation patterns of different array antenna configurations. Mutual coupling level of the antenna is investigated by varying the distance between the inter-element at resonant frequency. The transmission coefficient results shown in Figs.10,11 and 12. The antenna array are plotted with different distances between Antipodal Vivaldi antenna. The above results as in Table II show that the mutual coupling level is increased with decrease of the distance between the inter-element.

In Fig 13, the simulation results of mutual coupling levels with 0.3λ distance shows that there exist higher mutual

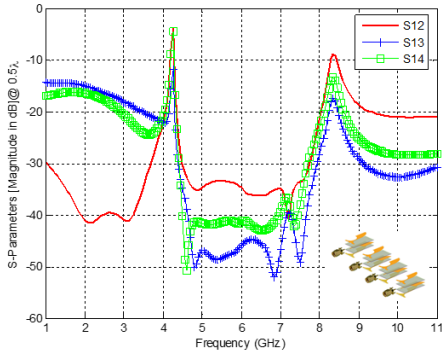


FIGURE 11. Parametric study of the broadband mutual coupling for different values of inter-element distance (0.5λ) (4 antennas array)

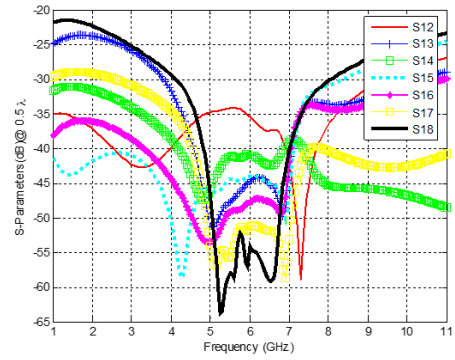


FIGURE 14. Parametric study of the broadband mutual coupling for different values of inter-element distance (0.5λ) (8 antennas array)

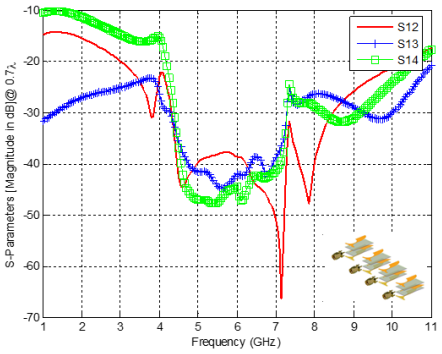


FIGURE 12. Parametric study of the broadband mutual coupling for different values of inter-element distance (0.7λ) (4 antennas array)

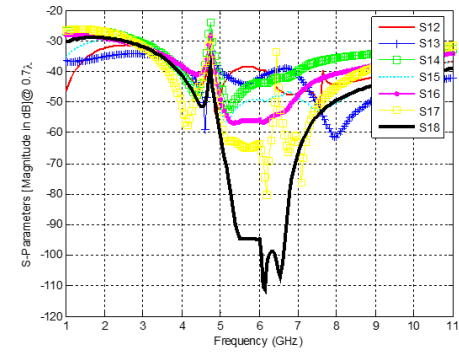


FIGURE 15. Parametric study of the broadband mutual coupling for different values of inter-element distance (0.7λ) (8 antennas array)

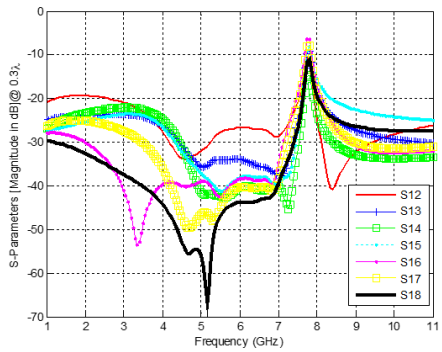


FIGURE 13. Parametric study of the broadband mutual coupling for different values of inter-element distance (0.3λ) (8 antennas array)

coupling levels between adjacent antipodal Vivaldi antenna. A parametric study of all design dimensions is also carried out. Figs.13,14 and 15 show the simulated S-parameters $S_{1i}(i = 2, \dots, 8)$ as a function of the distance between the

antipodal Vivaldi antenna. The distance between the antenna varied from 0.3λ to 0.7λ with step 0.2λ . Results show that with increasing the distance d , the coupling factor $S_{1i}(i = 2, \dots, 8)$ has gone up by limit and the curve moves upward with respect to the return loss (S_{11}) so we choose the distance $d = 0.5\lambda$. Note that, when we study the variation of any dimension, we fixed all other dimensions.

All stages of the Taguchi method are detailed in the references[26]-[27]-[31].

$$LD_1 = \frac{(\max - \min)}{s + 1} \quad (24)$$

where "max" and "min" are the upper and lower bounds of the optimization range, respectively. The fitness value is used to calculate the corresponding S/N ratio (η) in Taguchi's method through the following formula.

$$\eta = -20 \log(\text{Fitness}) \text{ (dB)} \quad (25)$$

$$\bar{\eta}(m, n) = \frac{1}{N} \sum_{i, OA(i, n)=m} \eta_i \quad (26)$$

$$\varphi_n|_{i+1}^2 = \varphi_n|_i^{opt} \quad (27)$$

For the $(i + 1)^{th}$ iteration.

$$LD_{i+1} = RR(i) \times LD_1 = rr^i \times LD_1 \quad (28)$$

TABLE 2. Mutual Coupling Comparison 8 Antipodal Vivaldi Antenna at 5.8 GHz

Distance (mm)	S_{12} level (dB)
0.3λ	-27dB
0.5λ	-34dB
0.7λ	-38dB

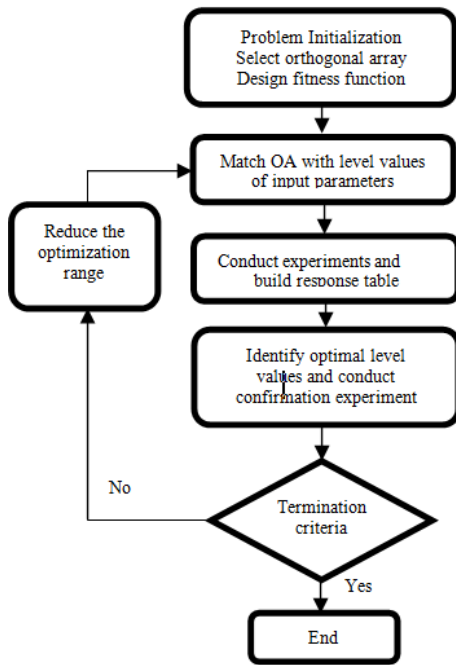


FIGURE 16. Flow chart of Taguchi method [26]-[27]

Where

$RR(i) = rr^i$ is called the reduced function.

$$\frac{LD_{i+1}}{LD_1} \leq cv \quad (29)$$

Where

cv is converged value.

B. NEURAL ARCHITECTURE

we have developed a technique for radiated lobe synthesis only from the excitation phases on each antenna array element. The Taguchi optimisation technique was used to synthesise directional lobes. The radiation pattern level can be controlled in each direction with lobe weighting coefficients. The developed technique has been tested on various types of directional lobes with zeros that can scan the entire angular range between -90 and 90. The computation time of this method is of the order of a few seconds, which makes this technique unsuitable for applications that require a very fast response such as the case of adaptive network or real-time adaptability applications. Hence the need to look for faster lobe formation techniques. In this paper we have used the neural technique especially RBF for the optimization of our parameters and learning which will be used later for the estimation of weights with which we can control our antennas in an intelligent way. For more details, we expose the neural model adopted in our own modelling approaches, which is the RBF neural network, and the learning base that is elaborated from the results provided by the synthesis method. The parameters taken into account in our learning base are

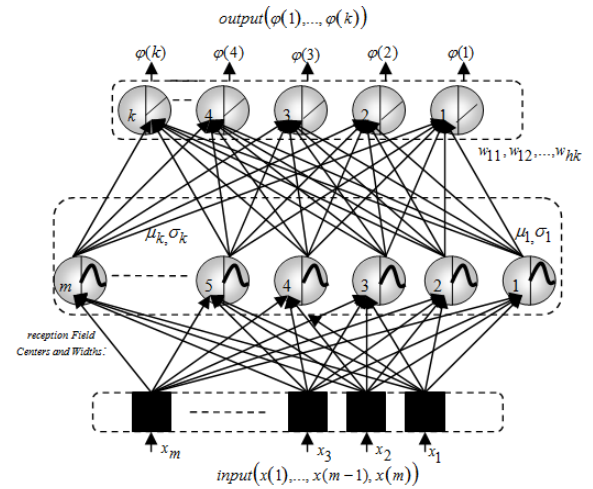


FIGURE 17. A sample three-layer RBF neural network

only the inter-element phase shifts according to the desired lobe. The efficiency of this model is represented by its ability to predict the non-linear behaviour of the synthesised values and by its speed of convergence. The capacity of neural network modelling is evaluated through its comparison with classical methods.

An RBF is a real-valued function whose value depends only on the distance from its receptive field center μ to the input x . It is a strictly positive radially symmetric function, where the center has the unique maximum, and the value drops off rapidly to zero away from the center. When the distance between x and μ (denoted as $\|x - \mu\|$) is smaller than the receptive field width, σ the function has an appreciable value. A typical RBF neural network has a three-layer feed-forward structure. The first layer is the input layer, which passes inputs to the (second) hidden layer without changing their values. The hidden layer is where all neurons simultaneously receive the n -dimensional real-valued input vector. We made use of the Gaussian basis function as it is one of the most popular choices for employment in RBF networks. We are taking 8 Antipodal Vivaldi antenna and change their phased difference and spacing between them and collect the data for 0 to 10 deg. These data used for the training of radial basis neural network and trained it over 0 to 10 deg in the spacing of 0.3, 0.5 and 0.7 wavelength. The efficiency of the training is dependent on the training parameters. We are using directivity of array pattern in the neural modeling.

$$R_j(x) = \exp\left(\frac{-\|\Phi - \mu_j\|^2}{2\sigma_j^2}\right) \quad (30)$$

Usually the distance is the Euclidean distance between x and μ . The actual output is directivity of radiation pattern in a particular direction. We collect the data for the best combination for phase angle with the spacing of 0.5, 0.6 and 0.7 wavelength, and uses -85 to 85 deg for the training. After the training we test the data with the ideal result. The detail result is given in Table IV.

TABLE 3. Optimum Phase values found by Taguchi-RBF Neural Networks

Element #	Example #1: Phase values			
	(deg.)@-75°	(deg.)@-45°	(deg.)@45°	(deg.)@75°
1	86.9760	63.9813	-63.2451	-86.7019
2	-99.0738	-168.0541	170.2666	99.8978
3	74.8746	-40.0881	43.7799	-73.5060
4	-111.1735	87.8764	-82.7084	113.0919
5	111.1735	-87.8764	82.7084	-113.0919
6	-74.8746	40.0881	-43.7799	73.5060
7	99.0738	168.0541	-170.2666	-99.8978
8	-86.9760	-63.9813	63.2451	86.7019

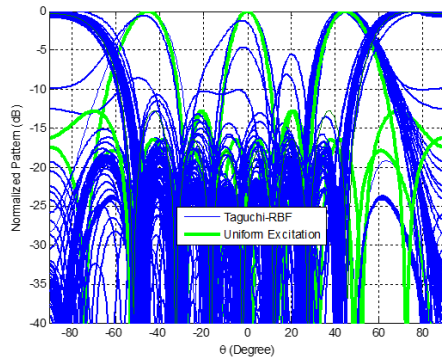


FIGURE 18. Radiation patterns of 8 Antipodal Vivaldi antenna@-75°,-45° , 0°, 45°, 75° and frequency 5.8 GHz.

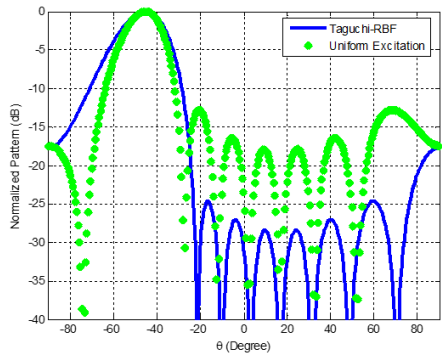


FIGURE 19. Radiation patterns of 8 Antipodal Vivaldi antenna@-45° and frequency 5.8 GHz.

The output can be expressed as $\varphi = [\varphi(1), \dots, \varphi(k)]$ with φ as the output of the i th neuron given by

$$\varphi_i = \sum_{j=1}^h w_{ji} R_j(x), i = [1, \dots, k] \quad (31)$$

In this example, Taguchi-RBF Neural Networks method will be applied on a 8-element linear array. Table III (Phase synthesis values) hold the optimum values of the phase obtained after 100 iterations[29-30].

The operation of the model is based on the prediction of the output after training (learning from the data set). The dataset for training RBF are collected from calculating theoretical phases using Taguchi-RBF Neural Networks. In MATLAB environment and after successful data training we test it, by

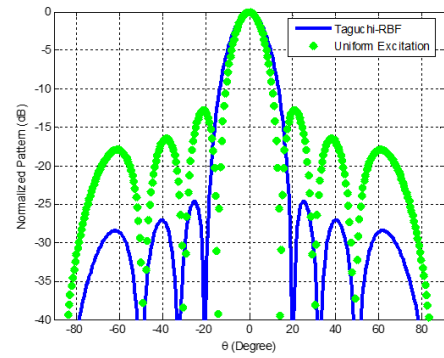


FIGURE 20. Radiation patterns of 8 Antipodal Vivaldi antenna@0° ,and frequency 5.8 GHz.

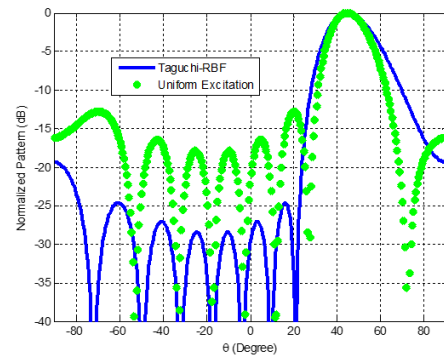


FIGURE 21. Radiation patterns of 8 Antipodal Vivaldi antenna@45° and frequency 5.8 GHz.

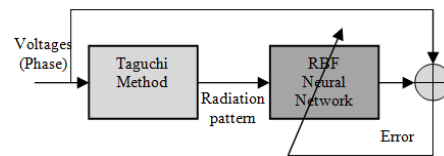


FIGURE 22. Neural network training procedure.

giving some data. The results presented in Figs. 18 to 21 show simulation radiation patterns with Side Lobe Level SLL (at -25dB), while maintaining main lobes in the direction of useful signal (at -75° to 75°) for 8 Antipodal Vivaldi antenna by Taguchi-RBF method when the main beam pattern steers at 75°,45°,-0°,-75° and -45°.Fig. 22 presents the Neural network training procedure between RBF neural networks and Taguchi method.

TABLE 4. Training Data (Taguchi-RBF Neural Networks)

Parameter	Value
Total Number neuron	50
Number of hidden layer	1
Learning rate	0.001
Goal	0.0002

IV. CONCLUSION

In this paper radial basis neural network based model are applied to predict radiation pattern in a particular phase angle with mutual coupling. The RBFNN model is inherently one type of general regression, which used to predict new results nonlinearly from some training data sets. The results obtained by the Taguchi-RBF modeling are in excellent agreement with the simulation results. An Antipodal Vivaldi antenna with enhanced radiation characteristics for UWB applications is presented in this paper by using Taguchi-RBF method. Patterns of 8-Antipodal Vivaldi antenna are discussed with the selection of the elements using a RBF-Taguchi linear array pattern design and analysis is essential for multiple beam forming technique for antenna design. RBF have better learning ability, generalization, parallel processing and error endurance attributes that lead to perfect solutions in applications where one needs to model the nonlinear mapping of complex data. This approach makes use of Neural Network and Taguchi that can be trained for any number of elements, spacing and excitation. Once the network is trained, it can find the parameters with respect to the input. Gain and half power beam width are the output parameters. The designed model of RBFNN has given quick speed of convergence and improved accuracy.

ACKNOWLEDGMENT

The authors would like to thank the Deanship of scientific Research at Umm AL-Qura University for supporting this work by Grant code (22UQU4361156DSR02)

ABBREVIATIONS

RBF: Radial Basis Function

HFSS: High-Frequency Structure Simulator

UWB: Ultra Wideband

PSO: Particle Swarm Optimization

GA: Genetic Algorithms

ANN: Artificial Neural Network

EPs: Evolutional Programming

RBFNN: Radial Basis Function Neural Network

REFERENCES

- [1] H. L. Shun and Hon H. Tat, "Decoupling Methods for the Mutual Coupling Effect in Antenna Arrays: A Review", *Recent Patents on Engineering*, pp 187-193, 2007
- [2] H. L. Shun and Hon H. Tat, "Mutual Coupling Compensation for Direction-of-Arrival Estimations Using the Receiving-Mutual-Impedance Method", *Hindawi Publishing Corporation International Journal of Antennas and Propagation*, Vol. 2010.
- [3] M. Wang, W. Wu, and Z. Shen, "bandwidth enhancement of antenna arrays utilizing mutual coupling between antenna elements", *Hindawi Publishing Corporation International Journal of Antennas and Propagation*, Vol. 2010
- [4] E. Saenz, K. Guven, E. Ozbay, I. Ederra, and R. Gonzalo, "decoupling of multifrequency dipole antenna arrays for microwave imaging applications", *Hindawi Publishing Corporation International Journal of Antennas and Propagation*, Vol. 2010
- [5] D. Ramamoorthy, "Impact of Mutual Coupling among Antenna Arrays on the Performance of the Multipath Simulator System", *Master's Thesis in Electronics*, January 2014
- [6] N. Damavandi and S. Safavi-Naeini, "Antenna optimization using a hybrid evolutionary programming method," in *Proceedings of the IEEE Antennas and Propagation Society International Symposium and USNC/URSI Meeting*, pp. 65–68, Washington, DC, USA, July 2005.
- [7] A. Hoorfar, "Evolutionary programming in electromagnetic optimization: a review," *IEEE Transactions on Antennas and Propagation*, vol. 55, no. 3, pp. 523–537, 2007.
- [8] R. L. Haupt, "Thinned arrays using genetic algorithms," *IEEE Transactions on Antennas and Propagation*, vol. 42, no. 7, pp. 993–999, 1994.
- [9] M. Donelli, S. Caorsi, F. de Natale, M. Pastorino, and A. Massa, "Linear antenna synthesis with a hybrid genetic algorithm," in *Proceedings of the Electromagnetics Research*, PIER' 04, pp. 1–22, 2004.
- [10] K. V. Deligkaris, Z. D. Zaharis, D. G. Kampitaki, S. K. Goudos, I. T. Rekanos, and M. N. Spasos, "Thinned planar array design using boolean PSO with velocity mutation," *Transactions on Magnetics*, vol. 45, no. 3, Article ID 4787361, pp. 1490–1493, 2009.
- [11] Z. Zaharis, D. Kampitaki, A. Papastergiou, A. Hatzigaidas, P. Lazaridis, and M. Spasos, "Optimal design of a linear antenna array under the restriction of uniform excitation distribution using a particle swarm optimization based method," *WSEAS Transactions on Communications*, vol. 6, no. 1, pp. 52–59, 2007.
- [12] N. Dipak, S. Shyam, S. Pattnaik et al., "Design of a wideband microstrip antenna and the use of artificial neural networks in parameter calculation," *IEEE Antennas and Propagation Magazine*, vol. 47, no. 3, pp. 60–65, 2005.
- [13] S. Lebar, Z. Guennoun, M. Drissi, and F. Riouch, "A compact and broadband microstrip antenna design using a geometrical-methodology-based artificial neural network," *IEEE Antennas and Propagation Magazine*, vol. 48, no. 2, pp. 146–154, 2006
- [14] D. I. Karatzidis, T. V. Yioultsis, and T. D. Tsiouklis, "Gradient-based adjoint-variable optimization of broadband microstrip antennas with mixed-order prism macroelements," *AEU - International Journal of Electronics and Communications*, vol. 62, no. 6, pp. 401–412, 2008
- [15] R. Haupt, "Comparison between genetic and gradient-based optimization algorithms for solving electromagnetics problems," *IEEE Transactions on Magnetics*, vol. 31, no. 3, pp. 1932–1935, 1995
- [16] S. H. He, W. Shan, C. Fan, Z. C. Mo, F. H. Yang, and J. H. Chen, "An improved vivaldi antenna for vehicular wireless communication systems," *IEEE Antennas and Wireless Propagation Letters*, vol. 13, pp. 1505–1508, 2014
- [17] F. Fioranelli, S. Salous, I. Ndiq, and X. Raimundo, "Through-the-wall detection with gated FMCW signals using optimized patch-like and Vivaldi antennas," *IEEE Transactions on Antennas and Propagation*, vol. 63, no. 3, pp. 1106–1117, 2015
- [18] J. D. S. Langley, P. S. Hall, and P. N. Newham, "Novel ultrawide-bandwidth Vivaldi antenna with low crosspolarisation," *Electronics Letters*, vol. 29, no. 23, pp. 2004–2005, 1993
- [19] R. Natarajan, J. V. George, M. Kanagasabai, and A. Kumar Shrivastav, "A compact antipodal Vivaldi antenna for UWB applications," *IEEE Antennas and Wireless Propagation Letters*, vol. 14, pp. 1557–1560, 2015
- [20] G. Teni, N. Zhang, J. Qiu, and P. Zhang, "Research on a novel miniaturized antipodal vivaldi antenna with improved radiation," *IEEE Antennas and Wireless Propagation Letters*, vol. 12, pp. 417–420, 2013
- [21] A. M. De Oliveira, M. B. Perotoni, S. T. Kofuji, and J. F. Justo, "A palm tree antipodal vivaldi antenna with exponential slot edge for improved radiation pattern," *IEEE Antennas and Wireless Propagation Letters*, vol. 14, pp. 1334–1337, 2015
- [22] H.-S. Lui, H. T. Hui, and M. S. Leong, "A note on the mutual-coupling problems in transmitting and receiving antenna arrays," *IEEE Antennas and Propagation Magazine*, vol. 51, no. 5, pp. 171–176, Oct 2009
- [23] W. L. Stutzman and G. A. Thiele, *Antenna Theory and Design*. New York: John Wiley Sons, 2012
- [24] S. Wang, X. D. Chen and C. G. Parini, "Analysis of Ultra Wideband Antipodal Vivaldi Antenna Design," *IEEE Loughborough Antennas and Propagation Conference*, 2-3 April 2007, Loughborough, UK, 2007.
- [25] D.H. Schaubert et al, "Wide bandwidth Vivaldi antenna arrays - some recent developments," *Proceedings of EuCAP 2006*, 6-10 November 2006
- [26] Weng, W., F. Yang, and A. Elsherbeni, "Linear antenna array synthesis using Taguchi's method: A novel optimization technique in electromagnetics," *IEEE Trans. on Antennas and Propagation*, Vol. 55, 723-730, 2007
- [27] Weng, W. C., F. Yang, and A. Elsherbeni, "Electromagnetics and Antenna Optimization Using Taguchi's Method", *Morgan Claypool*, San Rafael, CA, 2007

- [28] J. N. Sahalos, "Orthogonal Methods for Array Synthesis: Theory and the ORAMA Computer Tool", *John Wiley Sons*, 2006
- [29] Liodakis G., Arvanitis D., and Vardiambasis I.O., "Neural network – based digital receiver for radio communications", *WSEAS Transactions on Systems*, vol. 3, iss. 10, pp. 3308-3313, Dec 2004
- [30] A. Rawat, R. N. Yadav, and S. C. Shrivastava, "Application of Neural Network in Dynamically Phased Arrays Smart Antennas: A Review," *International journal of Electronics and Communication Engineering (AEU Elsevier)*, vol. 66, pp. 903-912, Nov. 2012
- [31] A. Smida, R. Ghayoula, N. Nemri, H. Trabelsi, A. Gharsallah and D. Grenier, "Phased arrays in communication system based on Taguchi-neural networks," *International Journal of Communication Systems*, vol. 27, 2013
- [32] K.S. Vishvakseenan, K.Mithra,R.Kalaiarasan and K. Santhosh Raj,"Mutual Coupling Reduction in Microstrip Patch Antenna Arrays Using Parallel Coupled-Line Resonators,"*IEEE Antennas and Wireless Propagation Letters*, vol.16, pp 2146 - 2149 vol. 27,2017
- [33] H.Liu, W. Wang, D.Tang, L. Zhang, Y.Wang and E. Miao,"Thermal Deformation Modeling for Phased Array Antenna Compensation Control", *MDPI Sensors*, , 2022.
- [34] Hayashi, I.; Higuchi, R.; Yokozeki, T.; Aoki, T. "Analytical study on the thermal deformation of ultralight phased array antenna", *Acta Astronaut*, 2021
- [35] S. Lou, W.Wang, H.Bao, N.Hu, G.Ge, X.Hu, S.Qian, and C.Ge,"A compensation method for deformed array antennas considering mutual coupling effect", *IEEE Antennas and Wireless Propagation Letters*, vol.17, no. 10, pp.1900-1904, Oct. 2018.
- [36] Ibrahim, A.A.; Ali, W.A.E., " High Gain, Wideband and Low Mutual Coupling AMC-Based Millimeter Wave MIMO Antenna for 5G NR Networks", *AEU Int. J. Electron. Commun.*, 2021, 142, 153990.
- [37] S. Zhu, H. Liu, Z. Chen and P. Wen, , "A compact gain-enhanced Vivaldi antenna array with suppressed mutual coupling for 5G mmWave application", *IEEE Antennas Wireless Propag. Lett.*, vol. 17, no. 5, pp. 776-779, Mar. 2018.
- [38] A. Kianinejad, Z. N. Chen and C.-W. Qiu, , "Full modeling loss reduction and mutual coupling control of spoof surface plasmon-based meander slow wave transmission lines", *IEEE Trans. Microw. Theory Techn.*, vol. 66, no. 8, pp. 3764-3772, Aug. 2018.
- [39] S.Jing, W.Guobin, Y.Lizhi, G. Xingchen, , "Simulation and Experimental Studies for the Active Reflection Coefficient of Phased Array Antenna on Mutual Coupling",*Journal of Microwaves*,2019. Vol.35
- [40] A.M. Oliveira; A.M.Neto; M.B.Perotoni, S.André.; N. Nurhayati and H. Baudrand "A Fern Antipodal Vivaldi Antenna for Near-Field Microwave Imaging Medical Applications",*IEEE Transactions on Antennas and Propagation*, vol. 69, non. 12, pp. 8816-8829, Dec. 2021